**Technical Report**
RAL-TR-1998-073



# A Prototype Gas Microstrip Wide Angle X-Ray Detector

**J E Bateman et al**

11th November 1998

COUNCIL FOR THE CENTRAL LABORATORY OF THE RESEARCH COUNCILS

Enquiries about copyright, reproduction and requests for additional copies of this report should be addressed to:

The Central Laboratory of the Research Councils
Library and Information Services
Rutherford Appleton Laboratory
Chilton
Didcot
Oxfordshire
OX11 0QX
Tel: 01235 445384 Fax: 01235 446403
E-mail library@rl.ac.uk

**ISSN 1358-6254**

RAL-TR-1998-073

# A PROTOTYPE GAS MICROSTRIP WIDE ANGLE X-RAY DETECTOR

J E Bateman, J F Connolly, G E Derbyshire, A S Marsh, R Stephenson,
J E Simmons and E J Spill
Rutherford Appleton Laboratory, Chilton, Didcot, OX11 0QX, U.K.

R C Farrow, W I Helsby and B R Dobson,
Daresbury Laboratory, Daresbury, Cheshire, WA4 4AD, U.K.

R Mutikainen[+] and I Suni
VTT Electronics, P O Box 1101, 02044VTT, Espoo, Finland

**Abstract**

A prototype high rate position sensitive detector for Wide Angle X-ray Scattering (WAXS) studies has been constructed and tested on beamline. The detector uses gas microstrip technology and allows for both high spatial (angular) resolution and high data rate to be achieved. The detector has the capability to be used over a wide range of X-ray energies (1 to 50keV) and to achieve detected and processed photon rates in the range of MHz per strip (0.4mm) with excellent detection efficiency. Typical of this detector technology is an energy resolution of better than 16% at 6keV, which offers the possibility of energy discrimination on a photon by photon basis. The detector has been built on a modular basis for ease of support and expandabilty. The results of a demonstration using polymer samples on the SAXS / WAXS station 8.2 at the Daresbury Laboratory Sychrotron Radiation Source are presented.

+

[+] Now at VTI-Hamelin Oy, P O Box 27, FIN-01621 Vantaa, Finland

## 1. Introduction

There is a continuing and increasing requirement for fast, efficient, one dimensional x-ray detectors for application in x-ray diffraction studies. This is true both for improving laboratory based sources and the increasing flux offered by synchrotron radiation sources. Gas detectors of various configurations have been developed in recent years to exploit the advantages and minimise the draw-backs of gas counter technology. The high counting rate capability of the multi-wire proportional counter (MWPC) has been exploited in the linear detector developed at Daresbury Laboratory [1] and the possibility of a curved detector (to avoid the parallax error induced by the necessarily thick gas volume) exploited in the INEL blade detector [2]. The advent of the gas microstrip detector (GMSD) [3] in which the detector electrodes are produced lithographically on a glass plate offers new options in the design of position sensitive x-ray counters [4]. In particular, the extensive development effort carried on at Rutherford Appleton Laboratory [5] and many other laboratories to perfect the technology of high spatial resolution, high counting rate devices for application in Particle Physics has resulted in a very impressive level of stable performance from GMSDs which can be adapted directly to applications in x-ray diffraction.

A generic problem with imaging gas counters arises from the low density of the gas converter which enforces considerable active depths (several centimeters) if a useful efficiency is to be achieved without the difficulties of hyperbaric operation. The long resulting drift paths cause parallax errors (if the detector is planar) and serious diffusion spreading of the electron clouds, both of which degrade the spatial resolution. The lithographic production of the electrode structure on a rigid surface makes possible a design in which the anode tracks point radially at the crystal target and the scattered x-rays travel through an extended gas space parallel to the anodes allowing an indefinite length of converter gas without parallax errors. When an x-ray converts in the gas the resulting cloud of electrons is drawn down onto the anodes through a distance typical of the aperture used in the azimuthal direction i.e. of the order of a few millimeters. This design means that large conversion depths can be accomodated with minimal diffusion spreading. A further advantage is that the small drift distances reduces the effects of electron attachment so relaxing constraints on the gas mixtures which can be used. It is therefore envisaged that for regular use premixed gas would be an option.

The "pointing anode wire" approach has been used successfully in an MWPC device for medical imaging [6] however, the lithographic process permits the implementation of the technique on a sub-millimeter scale of anode spacing which is impossible to achieve with wires. Another advantage of the GMSD over standard wire technology is its very high rate capability: count rate densities of $2.5 \times 10^5$ Hz/mm$^2$ for 8keV x-rays have been demonstrated with negligible gain drop [7]. The "pointing anode" design further enhances the rate capability of the detector by spreading the incident counting rate along several tens of millimeters of anode.

In order to exploit the potential of the MSGD to deliver several MHz of counting rate from every anode it is necessary to instrument each anode with an independent electronic channel capable of digesting this rate and storing the counts in a dedicated scaler for readout at the end of the exposure. The provision of this data capture system

is a significant part of the cost of the overall system; however, as each channel is identical and of a fairly simple design, the potential for implementation, of part or all, in monolithic silicon is obvious. The use of a simple counting system with appropriate control system allows for a high degree of timing resolution which is necessary for the increasing demands placed by dynamic scattering and diffraction synchrotron experiments.

## 2. The Detector

Figure 1 shows a photograph of the prototype detector with the drift electrode removed to expose the gas microstrip plates. The detector is based on a standard module of gas microstrip plate in which all the anode strips point at the target position placed at a radius of 200mm from the inside edge of the 50mm long anode strips. X-rays from the target travel throught the drift space parallel to the plate surface and the anode strips. As shown in figure 2, electrons generated by x-ray induced ionisation are drifted down onto an anode strip (following a path at right angles to the incident x-ray direction). Each plate subtends an angle of 15° at the target and each detector strip (0.4mm at the inside edge) subtends an angle of 2mrad at the crystal. (There are 128 strips per 15° sector.) The 10μm (constant width) anodes and interleaved cathode strips (variable width) are produce in a gold process on Schott S8900 glass. The anode strips are independently instrumented with amplifier, discriminator and scaler, the electrical connection being taken from the rear edge of the strips by means of wire bonding (figure 1).

The detector is extensible in θ up to 360° with no dead spaces since the plate joins take place in the middle of cathode strips. Preamplifier-driver cards are installed on the detector permitting the remainder of the electronics to be at a convenient distance from the detector. The detector aperture in φ is a relatively free parameter and will usually be constrained by experimental demands to a few mm. The drift electrode would generally be placed at ≈10mm and the placing of the beam relative to the plate controlled by collimation. The configuration of the electrostatic field in the drift region of the GMSD is such as to permit proper detection of x-rays to within 0.5mm of the plate surface.

Electronic readout of the anode strips is performed by means of dedicated preamplifiers mounted directly on the printed circuit board behind the GMSD plates (top of figure 1). Fabricated using surface mount components on a board with 16 channels [5] each preamplifier is capable of driving a pulse (typically 40mV for 8keV x-rays) down a terminated coaxial cable to the discriminator/scaler circuits which are housed remotely in a separate rack.

## 3. Detection Efficiency

The performance of a GMSD is not affected in any significant way by the length of the anode strip. Thus with this detector geometry one can achieve a large length of gas for the absorption of the x-rays without any attendant parallax errors. The anode length was chosen as 50mm for the prototype but the technology exists to produce 100mm

and 150mm lengths if required. Assuming that a very thin gas envelope window is used (the small φ dimension makes this possible) the main effective window is the "dead" drift space between the envelope window and the end of the anode strips. In the prototype device this is ≈10mm. (Figure 2) Figure 3 shows the detection efficiency of this set-up as a function of the linear absorption coefficient (μ) of the gas. The prototype exhibits an efficiency >50% for $0.2<\mu<0.7$ $cm^{-1}$ with a maximum of 58% at $\mu=0.35cm^{-1}$. Increasing the anode length to 100mm gives a maximum of 72% at $\mu=0.22cm^{-1}$ with efficiency>50% down to $\mu=0.08cm^{-1}$. An advantage of this property is that the detector efficiency can be tuned to any required x-ray energy above the envelope window cut-off by using the great flexibility of operation of the GMSD in respect of gas mixtures. Operation at the bottom end of the energy range will be determined by the window and at the top end by the absorption coefficient of xenon. Useful operation is thus possible from roughly 1keV to 50keV. Figure 4 shows the efficiency bands predicted for the prototype detector for typical gas mixtures based on 80% argon and 80% xenon with a hydrocarbon quencher (neglected in the calculations).

## 4. Energy Resolution

While energy spectrometry is not a primary aim with the detetector system proposed, it is important to maintain gain uniformity over the active area. The lithographic pattern used to achieve the "pointing anode" effect (often referred to as the "keystone" pattern) has been studied for application in Particle Physics [8] where it was found that the inevitable gain shifts induced by the change in the aspect ratio of the detector geometry along the pattern could be minimised (but not eliminated) by grading the anode-cathode gap width (G) with the pitch (P) (the cycle period of the whole pattern) according to the empirically determined formula:

$$G = \alpha P + \beta G_0$$

where P increases linearly with distance from the front edge of the detector. Choosing the far end (i.e. greatest radius of curvature) of the anode pattern for reference ($G_0$ = 145μm) we adopted the parameters $\alpha=1/6$ and $\beta=0.426$.

By equiping the protoype detector with a thin foil drift electrode and top window the gain could be measured as a function of radial position using a $^{55}Fe$ x-ray source. The upper curve in figure 5 shows that there is a 24% end to end gain variation. When the source was collimated and injected along the beam direction this beam spread resulted in a FWHM energy resolution of 20.5%.

While this performance is tolerable for general application, a simple option exists to trim this gain variation further. A feature of the GMSD is that the drift field has a very weak effect on the gas gain. Thus by using a drift electrode divided radially into ring electrodes fed from a graded potential divider network it is possible to compensate for the radial gain variation. The lower curve in figure 5 shows the resulting "flat" radial gain distribution which has a residual RMS error of 2.66%. Figure 6 shows the $^{55}Fe$ pulse height spectrum for a radial beam with a FWHM of 15.3% which is the standard

value for an argon/isobutane gas mixture. The range of drift potential required to achieve this compensation (with a 10mm drift space) is approximately -1800V to -3300V. This difference in drift field will induce some variation in the lateral diffusion of the electron clouds (see discussion below) but since the diffusion versus field curve is very flat in most argon-based gas mixtures at fields of ≥1kV/cm (at 1bar) this is not a problem.

As will be discussed in the next section, lateral diffusion in the electron drift results in the sharing of the charge in an event between strips and the loss of a good energy spectrum in the anode channels. (Passing the beam within a mm or two of the plate surface very much reduces this effect by keeping diffusion to a minimum.) A good energy signal is always available on the cathode pads which automatically sum the signals from a number of strips. The cathode pads (groups of 16 in the prototype) are visible at the bottom edge of the plates in figure 1. If good energy resolution is called for the cathode pads can be instrumented and the signals from a discriminator used to gate the data acquisition.

## 5. Spatial Resolution

The angular resolution delivered by the detector is determined by the spatial resolution (in the θ direction) realised for an x-ray interaction in the detector convolved with the profile of the primary beam-sample interaction spread. The detector spatial resolution is governed by the interaction of the various physical processes of detection with the structure and readout of the detector.

### 5.1 Photoelectron range

The range of the x-ray-induced photoelectron is a rapid function of its energy and this is usually a significant contribution to the spatial resolution in a gas detector. At an xray energy of 8keV the measurements of Smith et al show that the contribution of this effect to the spatial resolution in argon is in the region of 0.28mm FWHM and in xenon 0.07mm FWHM [9].

### 5.2 Electron Diffusion

A point-like source of electrons generated in the drift space of the MSGD spreads out in a gaussian manner as it drifts toward the detector plate. The diffusion depends on the gas mixture used and the electric drift field and is characterised by the RMS ($\sigma$) of the transverse distribution of the electron cloud after a drift of 1cm. For most practical gas mixtures and drift fields this parameter lies in the range $0.05 < \sigma_0 < 0.4\text{mm/cm}^{-1/2}$ [10]. Noble gases with an alkane quencher show a flat minimum (with E-field) at about $0.2\text{mm/cm}^{-1/2}$. A broad beam (in $\varphi$) produces a superposition of gaussians with the resulting curves fitting quite well to a sum of two gaussians. Figure 7 shows the electron footprint distributions simulated by a montecarlo model for various beam depths (as measured from the plate surface) with this value of $\sigma_0$. In the case of a

10mm deep drift space the raw montecarlo data is shown as well as the double gaussian fit. At 8keV the electron range effects will broaden this distribution significantly in the case of the 2mm drift depth but scarcely at all in the case of a 20mm drift.

### 5.3 Models of Spatial Resolution

The spatial resolution delivered by any readout system depends on the way it treats the information encoded in the above electron distribution. In the ideal case with the ability to resolve every electron position as it arrived at the detector plane with infinite resolution and no noise the spatial resolution limit would be $\sigma_e/\sqrt{N_e}$ where $\sigma_e$ is the RMS of the electron distribution at the detection plane and $N_e$ is the number of electrons per event. In the case of a 2mm drift (8keV x-ray) this is $0.04/\sqrt{286}$ (= 2.36μm) and of a 20mm drift, $0.16/\sqrt{286}$ (=9.46μm). In the real world it is necessary to detect the arrival of the electron cloud in bins of finite width which dramatically degrades these numbers (in any case the electron range effects are more than an order of magnitude greater at 8keV).

In the simplest case the integrating bin is substantially wider than the electron footprint and the response of the readout is simply a top hat of which the RMS deviation is $W/\sqrt{12}$ (=0.29W) where W is the width of the bin. If the spatial sampling is significantly finer one can obtain a coarse footprint ($y_i$) of the electron footprint from which the mean position (X) can in principle be extracted and a spatial resolution much nearer the ideal achieved. Thus:

$$X = \frac{\Sigma x_i y_i}{\Sigma y_i} \qquad \text{with error} \quad \sigma_x^2 = \frac{\Sigma y_i (x_i - X)^2}{\Sigma y_i}$$

There are two distinct approaches to performing the required algorithm, analogue (delay line, resistive divide, capacitative divide) and digital (each signal is digitised and the mathematical algorithm calculated). The parameter of concern in determining the spatial resolution is $\sigma_x$ and it is immediately obvious from the formula that the amplitudes of the samples ($y_i$) on the wings of the distribution (where the signal to noise ratio is poor) make a large contribution to the sum of the squares. The noise in the $y_i$ comes from two sources, the amplifier noise and the poisson noise inherent in the quantised electron cloud. With adequate gas gain the former can be reduced in significance, however the poisson noise and avalanche gain fluctuations set an irreducible limit for error in the calculation of the mean position.

A montecarlo model was created to simulate the response of a typical GMSD to 8keV x-rays and assess the spatial resolution attainable with different methods of readout. Figure 8 shows the RMS resolution produced by the mean algorithm in strip-widths for a typical GMSD with a 0.3mm wide strip detecting 8keV x-rays from a 10mm drift space with the diffusion constant as the independent variable. The different curves represent the response with varying amounts of electronic noise which is expressed in terms of x-ray energy deposit in the counter. The poisson limit of $\sigma_x$ is reached with a

noise level of 0.01kev (SNR=800) and is seen to be about 0.07 stripwidths at the optimum $\sigma_0$ of 0.2mm/cm$^{-1/2}$. (It is a happy coincidence that the optimum $\sigma_0$ is found in most cases to correspond with a value that is readily obtainable in practice.)

With low noise figures the behaviour of $\sigma_x$ is readily comprehended in terms of the statistical model: as $\sigma_0$ approaches zero from above $\sigma_x$ approaches $1/\sqrt{12}$; increasing $\sigma_0$ brings the benefit of interpolation initially but as $\sigma_0$ continues to increase and spread the electrons ever more thinly, the noise moments increase $\sigma_x$.

With the low gain (1000) of the GMSD and the wide bandwidth of the fast amplifiers needed for the high counting rate applications in view, the SNR achieved with 8keV x-rays is in the region of 40, i.e. the noise is 0.2keV. Figure 8 shows that under these circumstances the best $\sigma_x$ obtainable from the mean algorithm is about 0.7 stripwidths or twice as bad as just counting a strip. (This plot largely explains why there have been no reports of successful readout of a GMSD using a delay line.)

With the narrow strip widths achievable in GMSD technology it is possible to consider the alternative approach of simply counting the signals in each strip above a discriminator. Naively one would expect $\sigma_x \approx 0.29$ and figure 8 shows that it is indeed so. Instead of evaluating the mean this model simply counts the pulses above a discriminator and evaluates the position error from all the hits (sometimes two adjacent channels will register). As figure 9 shows $\sigma_x$ is essentially constant (0.25) and independent of $\sigma_0$ at the very poor SNR of 20. The main concern in this readout is that if the charge footprint is too wide then efficiency is lost as no pulse is big enough to trigger a discriminator. However, with the strip width of the prototype (0.4mm) 100% is preserved up to a $\sigma_0$ of 0.2mm/cm$^{-1/2}$, which one can expect to achieve. $\sigma_x$ is slightly better than the simple model because events which share between adjacent strips give a little interpolation.

Taking the value of $\sigma_x$ at $\sigma_0$ = 0.2mm/cm$^{-1/2}$, $FWHM_x = 0.237*0.4*2.36 = 0.224$mm. Thus $FWHM_\theta$ = 1.12mrad and there are 936 FWHM in a four section (60°) detector.

It is important that there is a useful range of discriminator settings in which to operate. Figure 10 shows that at discriminator levels between 0.2 and 0.4 of the incident energy both the efficiency and the spatial resolution are constant.

The fact that one event can trigger two adjacent channels of readout makes the differential linearity of the readout sensitive to the gain uniformity in the channels. The model was used to check the effect of the inevitable fluctuations in gain between channels. Figure 11 shows the relative RMS induced in flood data as a function of the relative RMS imposed on the channel gains. The result is an amplification factor of 1.56. The RMS fluctuation in the channel gains has been observed to be around 2% which with the amplification should result in a differential non-linearity of 3%.

## 6. Counting Rate Performance

Counting rate limitations are set partially by the detector and partially by the electronics.

### 6.1 Rate-induced Gain Shifts

The positive ion clouds generated in a gas avalanche device reduce the amplifying fields at high rates and so the gain. Experience with GMSDs has shown that at count rate densities of 250kHz/mm$^2$ of 3x10$^5$ electron pulses (about the size with which the prototype operates with 8keV x-rays) there is a gain droop of 6% (figure 12) [7]. In the protoype detector events are spread (not perfectly uniformly) along 50mm of detector strip of 0.5mm width, i.e. ≈25mm$^2$ of plate. Thus the 6% gain droop is in the region of 6MHz for the whole anode. How much gain droop is acceptable will depend on the nature of the data being taken. This figure may be taken as an upper limit to what may be tolerable.

### 6.2 Event Occupancy

The pulse duration provided by the GMSD is less than 100ns and pulse pair resolution depends on the sophistication of the amplifier shaping and the discriminator (the pulse rise time is ≈10ns). With simple RC-CR shaping one can achieve 100ns pulse pair resolution.

### 6.3 Electronic Deadtime

The electronic deadtime associated with the capture of an event is largely a function of the sophistication of the discriminator and scaler. Since each channel is independent with no complicated logic it is hoped that simple circuits will suffice to achieve data capture at up to 5MHz per channel without excessive deadtime losses. The main complication is that each channel should have its own deadtime correction since the rates can vary dramatically over the counter aperture.

In summary, it is suggested that maximum data capture rates in a single channel should be in the region of a few MHz. Some of the rate capability is lost due to the fact that a fraction (depending on the threshold settings but typically 20-30%) of events will double count in adjacent channels. This is not expected to be noticable effect.

## 7. A Preliminary Test of the Prototype Detector

As a demonstration of its performance the prototype detetector was set up on the 8.2 Small Angle Scattering Facility beside the existing INEL detector at the DL Sychrotron Radiation Source [2] . An interface module was constructed to permit the on-board preamplifiers to drive the 200 channel data capture electronics of the DL MWPC Linear Detector system [1].

The detector was operated with a drift potential of -3500V, a cathode potential of -700V and the anodes at earth potential. A gas flow of 100cc/min of argon + 25% isobutane was maintained by means of a mass-flow system.

In order to normalise out the inevitable differential non-linearity of the multi-channel system a high-statistics flood of the detector was taken using a $^{55}Fe$ source and used for post-processing.

Figure 13 shows the response of the detector (normalised) to the diffraction pattern produced by a sample of high density polyethylene in a 100 second exposure with the full beam intensity. The global data acquisition rate was approximately 1.3Mhz. A gaussian fit to the large peak shows that the spatial resolution measured on the detector is 1.07mm (FWHM). Since mounting facilities for the detector were limited in scope much of this width is attributed to alignment error.

The value of the high data acquisition rate is illustrated by figure 14 which shows useful diffraction patterns acquired in intervals of 10ms and 1ms respectively.

Comparison with the data rates acquired by the INEL on the same sample indicates that the GMSD was taking data 3000 times faster. In practice the beam was incapable of driving the GMSD faster than a rate of 150kHz in the peak channel which is at least a factor of ten lower than the potential limit of the GMSD.

## 8. Conclusions

The extensive development carried out on the GMSD for Particle Physics applications predicted that it should present excellent potential as a detector for x-ray scattering applications. The test reported above shows that a detector with a very high rate capability can be realised. While the experimental set-up used was not sufficiently precise to demonstrate the limiting spatial resolution of the GMSD, we are confident that the detailed analysis of the ultimate spatial resolution described above will be verified in future tests.

The effectiveness of the tiling system used with the plates is demonstrated by the lack of any artefact at the join between the two plates (channel 128 to channel 129).

The detector proved simple and robust in operation. Experience in Particle Physics indicates that a very acceptable lifetime can be achieved with this system when care is taken with the gas supply [11].

## 9. Future Developments

The present protoype detector is intended as a demonstration of the potential of the GMSD in this application. Optimisation for particular applications will be able to capitalise on the flexibility of this design in various ways:

Experience on the beamline shows that it would be more practicable to increase the inner radius of 200mm by a factor of two. The readout granularity of the system can be relatively easily adjusted by leaving the basic pitch of the GMSD strips the same and bussing them on the mother circuit board as required. It is pointless to have spatial resolution in the detector significantly smaller than the beam width, so it is important to be able to tailor this to the beamline. The 15° module will in this case become a 7.5° module requiring 8 modules for a 60° aperture. Fortunately the cost of a production GMSD plate is not excessive and this will not be a problem.

Associated with the granularity of the readout is the issue of the provision of readout electronic channels. The electronic functions required per channel are relatively simple (preamplifier, shaper, discriminator, scaler) but large in number and lend themselves to implementation in monolithic silicon technology. A design program is under way to achieve this goal.

In future designs it is in principle possible to sweep the dead window space by using a carefully designed window held near the drift cathode potential to ensure that ionisation in that region is deposited on an anode. This modification will tend to push the detection efficiency towards 100% in the central band of x-ray energy.

GMSDs operate very well under hyperbaric conditions so that for high energy x-rays the use of pressurised xenon is a realistic option. (Keeping the φ window width down to a few mm makes this easier.) With a 150mm anode length and a few bars of xenon operation towards photon energies of 100keV is foreseeable.

**Acknowledgements.**

We would like to thank R Cernik, G Jones, G Diakun and B Komanshek and members of the SR Detector Group at Daresbury for their support and help with this project.

## REFERENCES

1. R A Lewis, C J Hall, B Parker, A Jones, W Helsby, J W Sheldon, P Clifford, M Hilton, N Fore, Nucl Instr & Meth A392 (1997) 42-46

2. W Bras, G E Derbyshire, A J Ryan, G R Mant, A Felton, R Lewis, C Hall and N Greaves, Nucl Instr & Meth A326 (1993) 587

3. A Oed, Nucl Instr & Meth A263 (1988) 351-359

4. V. Zhukov, F Udo, O Marchena, F G Hartjes, F D van den Berg, W Bras, E Vlieg Nucl Instr & Meth A392 (1997) 83-88

5. J E Bateman, J F Connolly, R Stephenson, M Edwards and J C Thompson, Nucl Instr & Meth A348 (1994) 372-377

6. E A Babichev, S E Baru, A G Khabakpashev, G M Kolachev, G M Savinov, L I Shekhtman, V A Sidorov and A I Volobuev, Nucl Instr & Meth A310 (1991) 449

6. E A Babichev, S E Baru, A G Khabakpashev, G M Kolachev, G M Savinov, L I Shekhtman, V A Sidorov and A I Volobuev, Nucl Instr & Meth A310 (1991) 449

7. J E Bateman and J F Connolly, Rutherford Appleton Laboratory report, RAL-93-096

8. ATLAS Internal Note, INDET-NO-076 (1994)

9. G C Smith, J Fisher and V Radeka, IEEE Trans Nuc Sci NS-31 (1984) 111

10. A Peisert and F Sauli, CERN report, 84-08

11. J E Bateman, J F Connolly, Yu N Pestov, L I Shekhtman, R Mutikainen and I Suni, Rutherford Appleton Laboratory report, RAL-94-114

## FIGURE CAPTIONS

1. This photograph shows the two GMSD plates installed in the prototype detector with the anodes bonded to printed circuit tracks leading to the on-board preamplifiers.

2. A schematic cross-section of the prototype detector showing the path of an incident x-ray and the subsequent drift paths of the photoelectrons towards the anodes of the GMSD.

3. The detection efficiency of the detector as a function of the linear x-ray absorption coefficient ($\mu$) of the gas filler for typical values of the window dead layer (w) and the active anode length (d).

4. The calculated detection efficiency bands of the prototype detector for argon and xenon gas mixtures. The absorption of the quencher is neglected.

5. The relative gain modulation (%) along the length of the anode strips - with a plain drift electrode (upper curve) and a graded drift electrode (lower curve).

6. The pulse height spectrum obtained with a radial beam of $^{55}Fe$ x-rays in the detector when fitted with the graded drift electrode.

7. Bi-gaussian fits to the montecarlo models of the lateral footprint of point-like distributions of photoelectrons after various drift distances (d). The montecarlo data is shown in the case of d=10mm.

8. The spatial resolution ($\sigma_x$, evaluated in strip widths) as calculated by the montecarlo model using the centroid method. The dependence of $\sigma_x$ on the diffusion properties of the gas ($\sigma_0$) and the electronic noise in the readout amplifiers ($E_{noise}$) is demonstrated in the case of 8keV x-rays and a 10mm drift.

9. The spatial resolution and trigger efficiency are modelled by the montecarlo as a function of the diffusion constant of the gas ($\sigma_0$) under the same signal to noise conditions as figure 8 in the case of strip-by-strip readout.

10. With the operating conditions of figure 9 the montecarlo model permits the assessment of the discriminator setting required in the strip-by-strip readout method to assure full trigger efficiency and optimum spatial resolution.

11. The montecarlo model permits a calculation of the variance induced in a flood field by the variance in the electronic channel gains. (This effect is a result of the signal sharing induced by the photoelectron diffusion.) The conditions of operation are listed on the graph.

12. The gain versus rate effect measured in a GMSD of similar specification to the prototype x-ray detector (10μm wide anodes in a 300μm pitch strip produced on S8900 glass) [7].

13. The diffraction pattern observed with the GMSD system in a 100s exposure on the 8.2 Small Angle Scattering Facility at DL when a sample of high density polyethylene was exposed.

14. The diffraction patterns observed with the GMSD system from the high density polyethylene sample with time apertures of 10ms and 1ms.

FIGURE 1

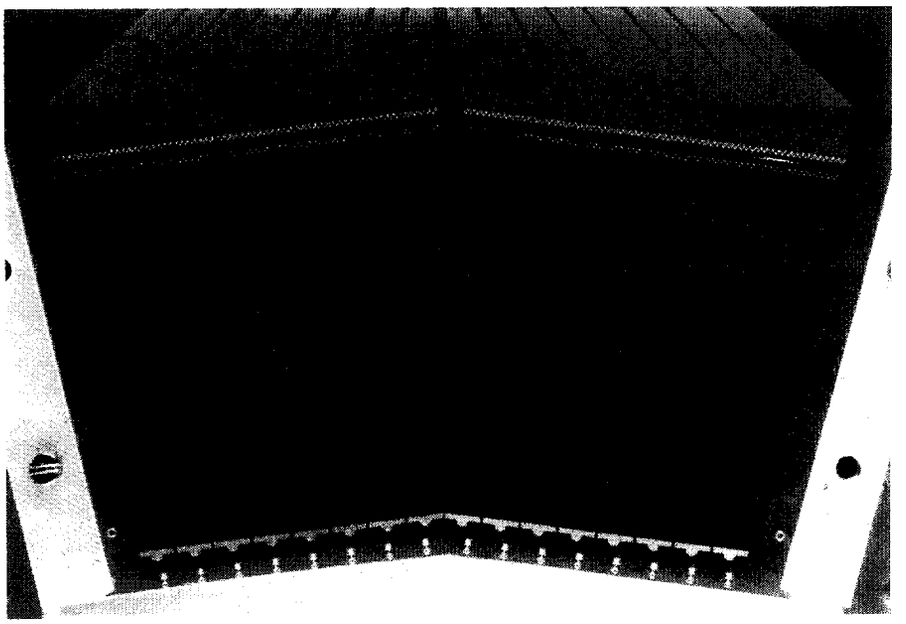

FIGURE 2

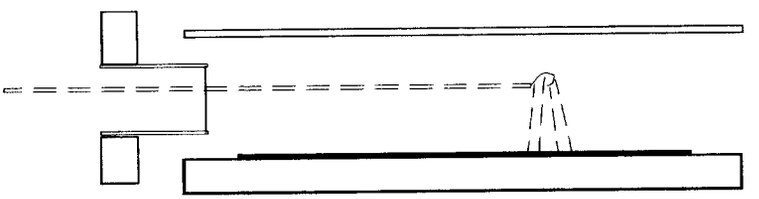

FIGURE 3

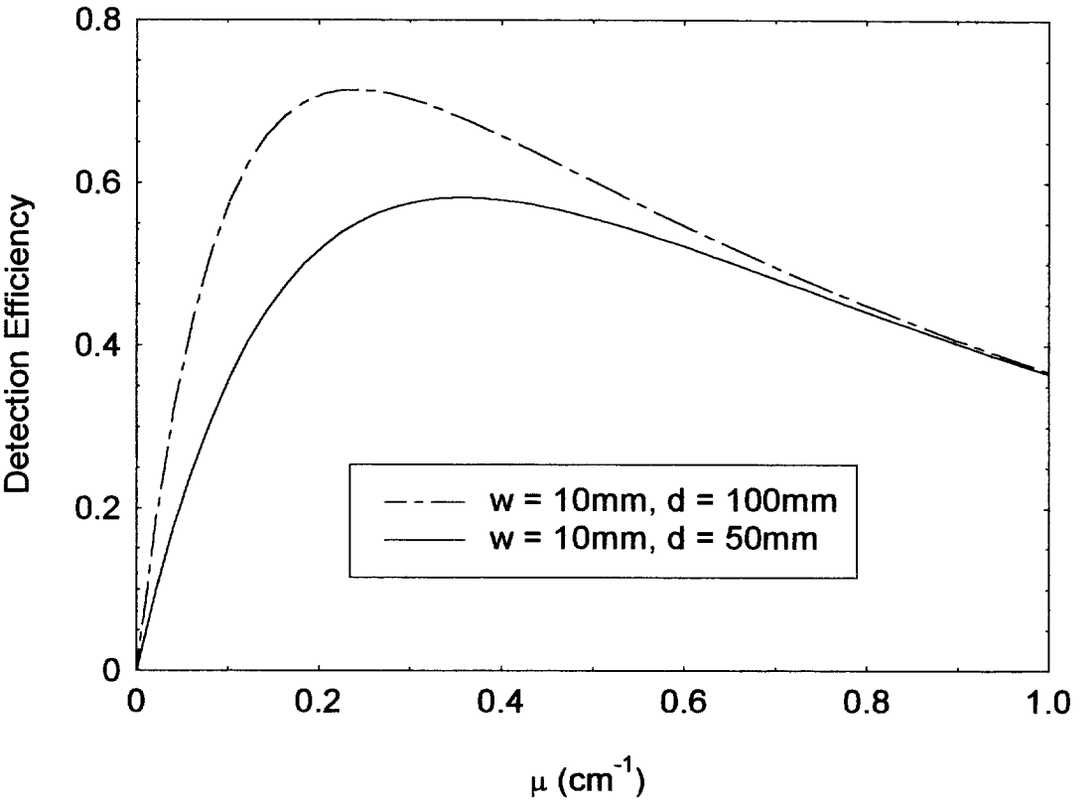


FIGURE 4

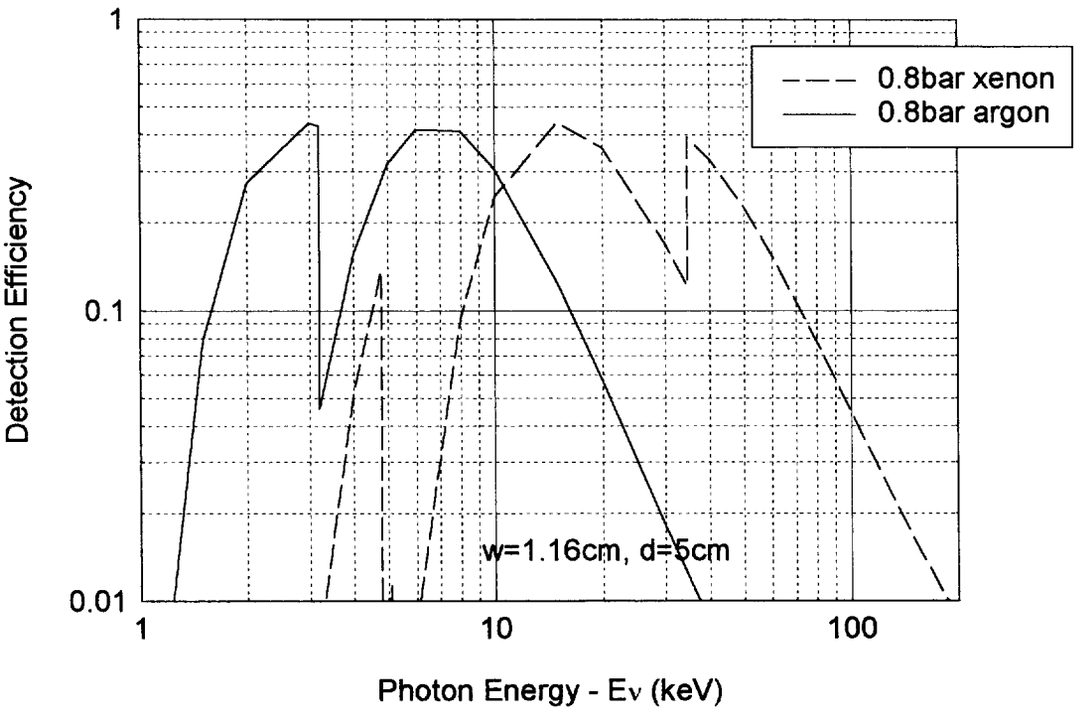

FIGURE 5

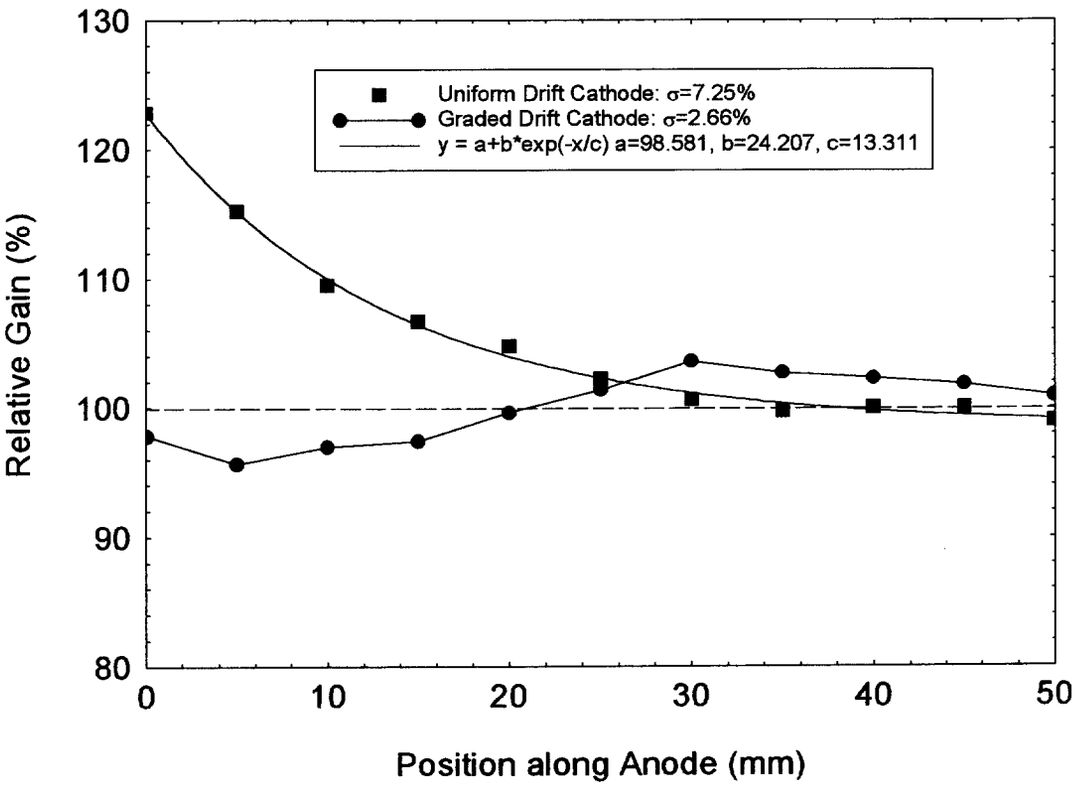


FIGURE 6

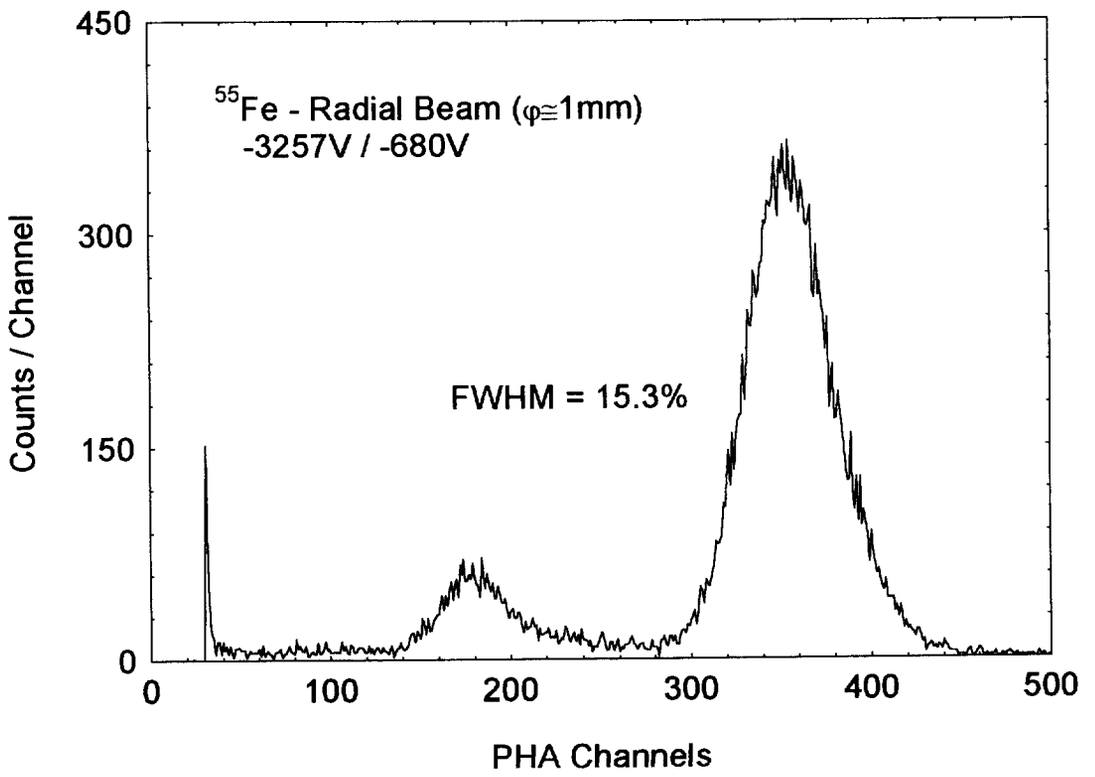

FIGURE 7

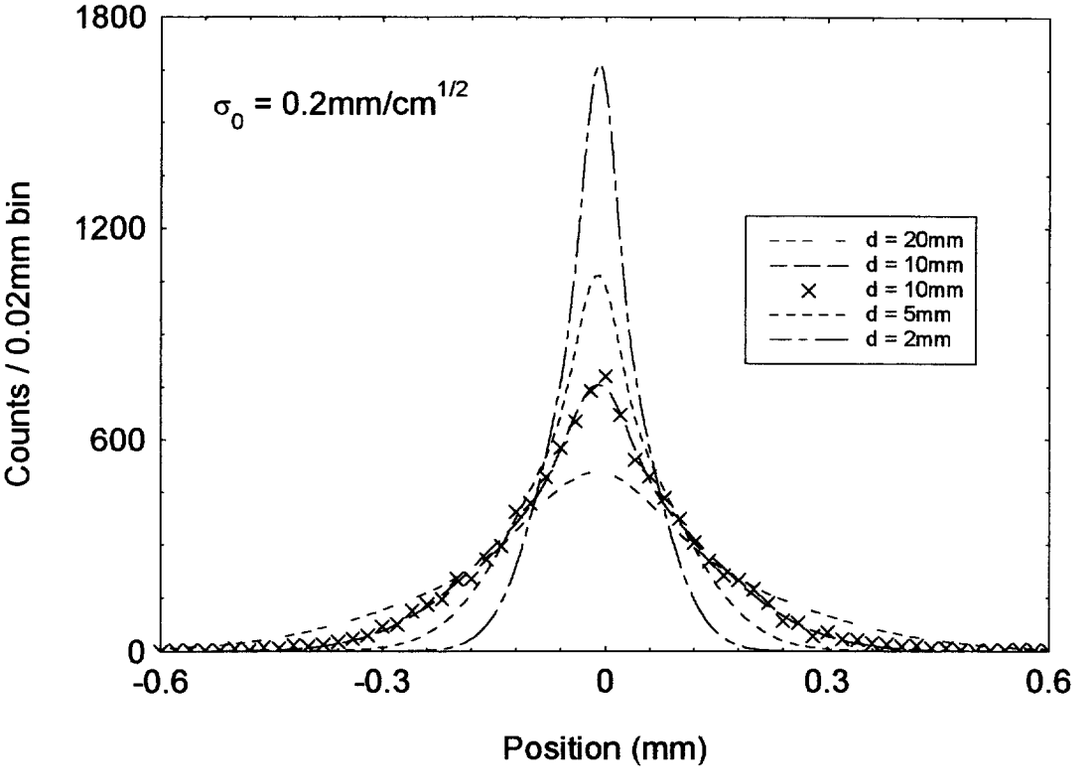


FIGURE 8

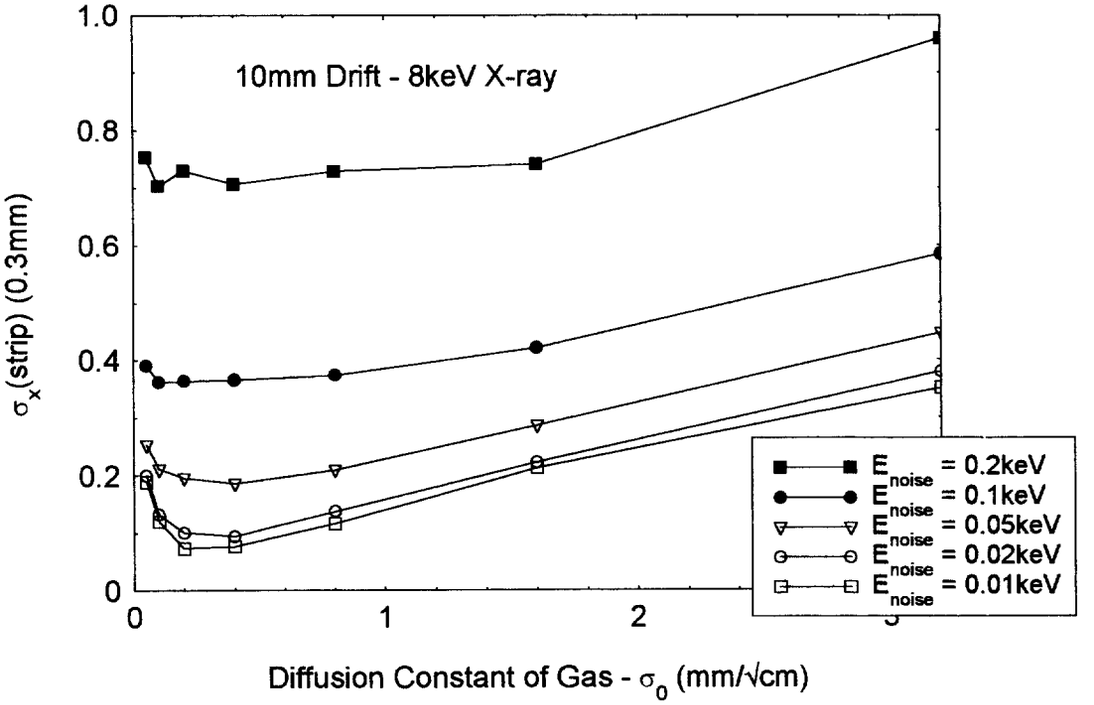

FIGURE 9

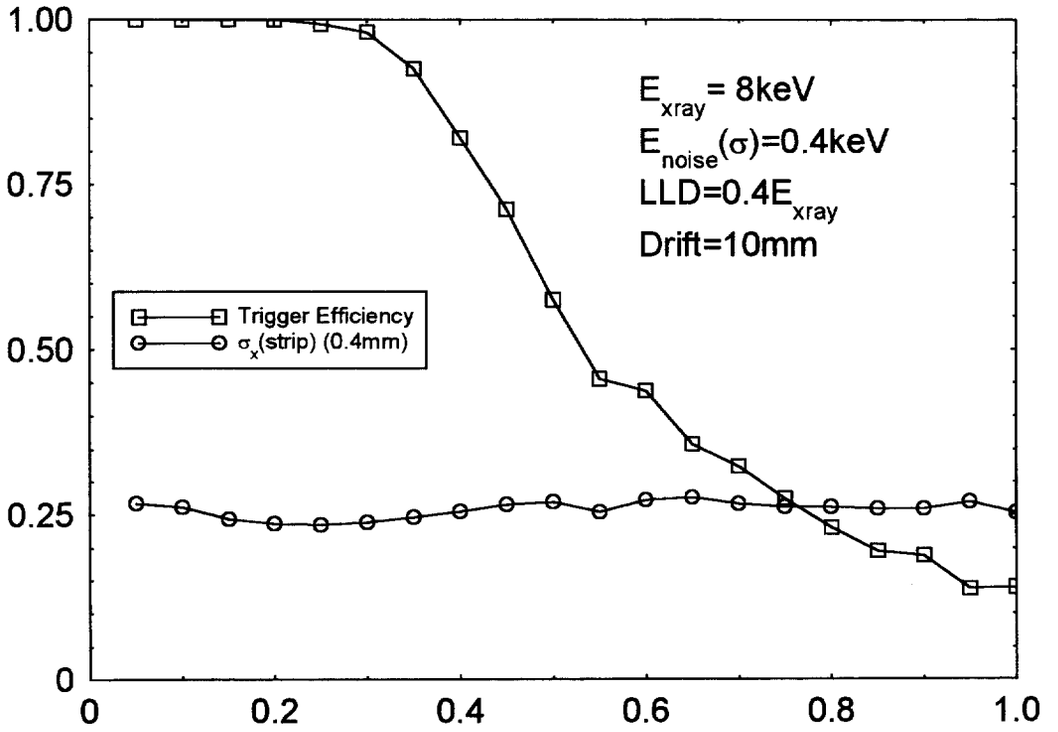


FIGURE 10

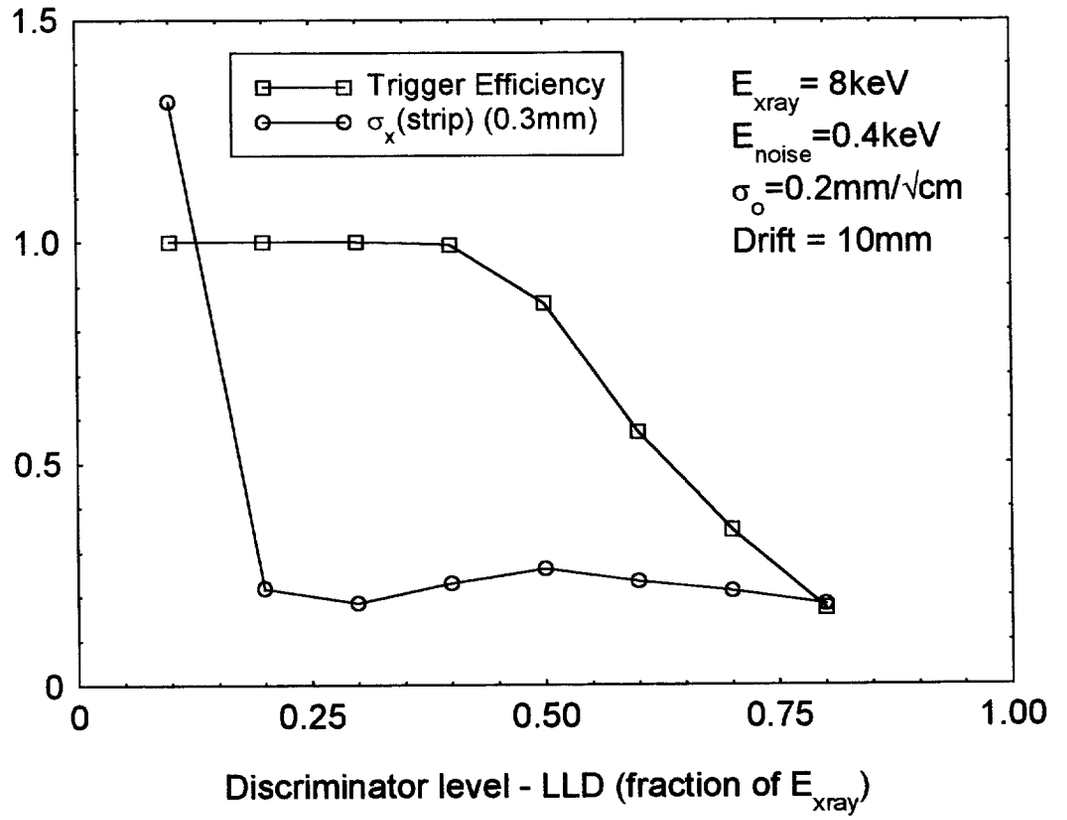

FIGURE 11

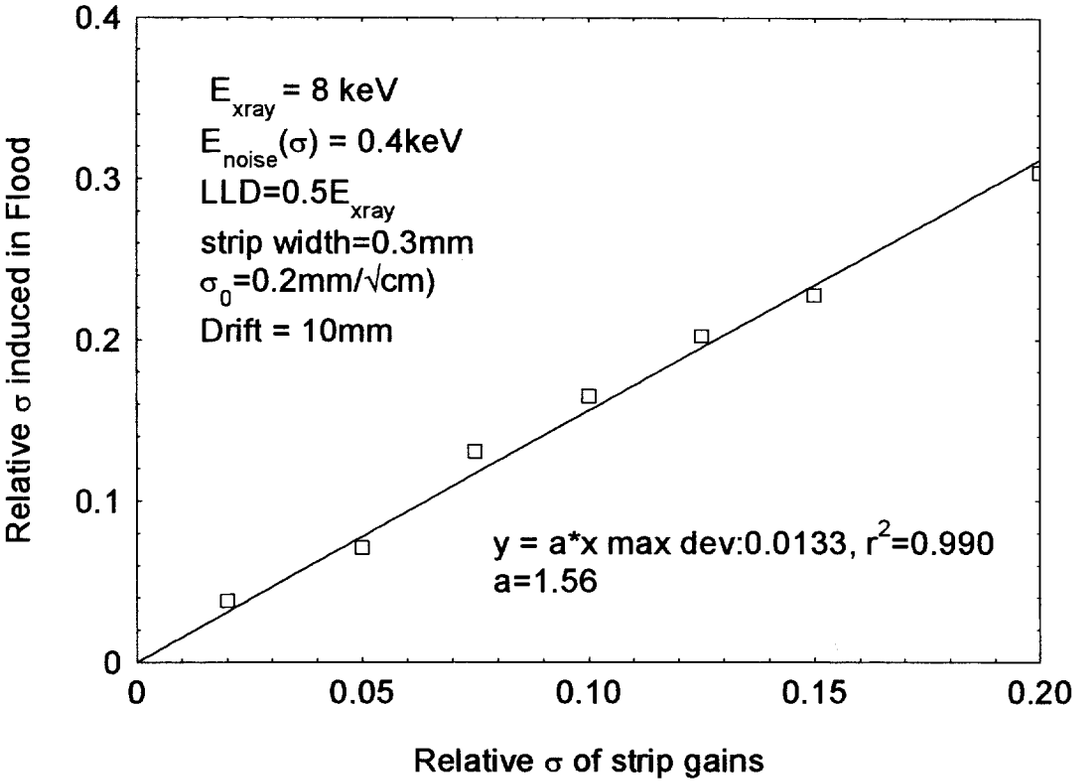


FIGURE 12

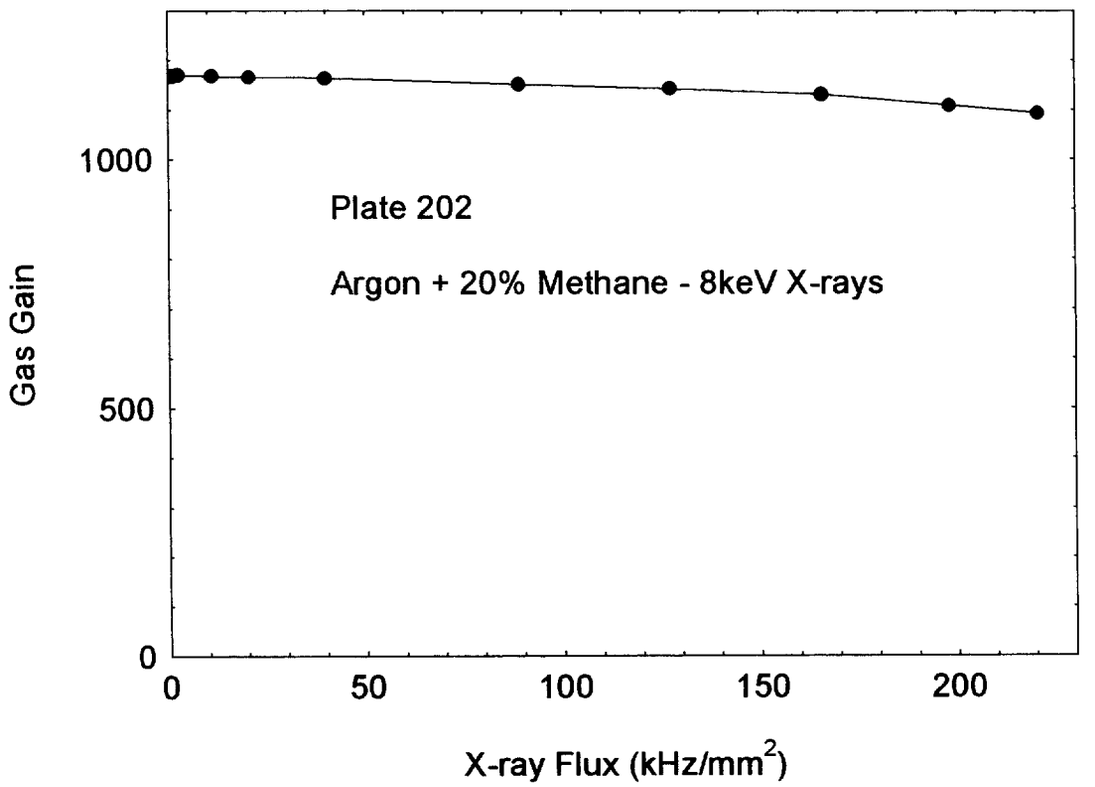

FIGURE 13

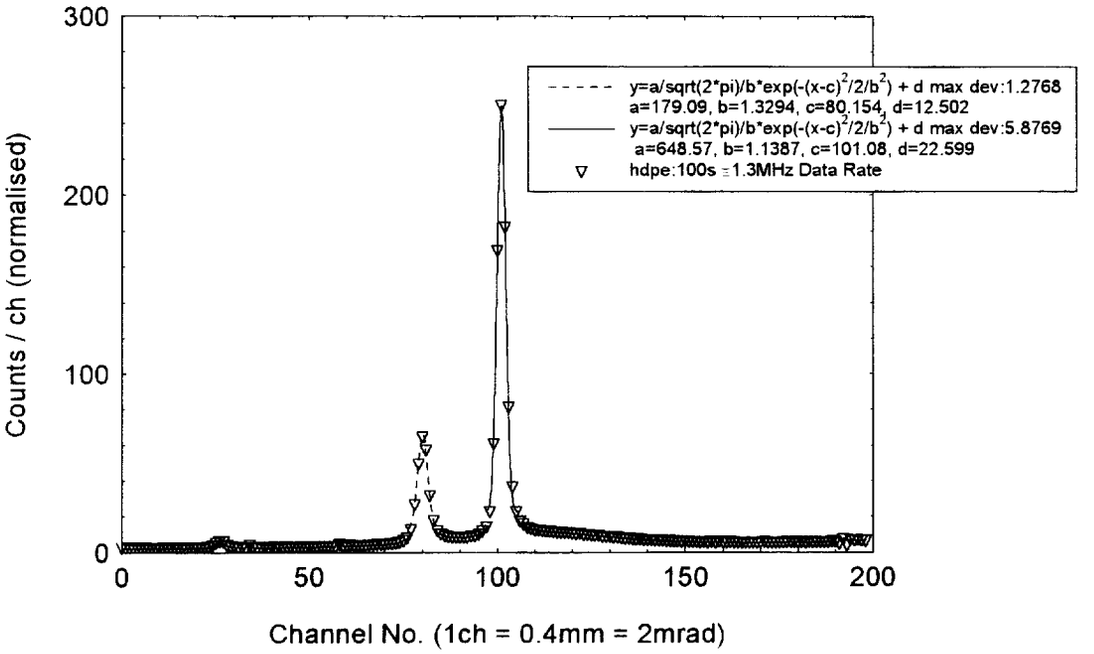


FIGURE 14